

# Classical dynamics of a nano-mechanical resonator coupled to a single-electron transistor

A. D. Armour

*School of Physics and Astronomy, University of Nottingham, Nottingham NG7 2RD, United Kingdom*

M. P. Blencowe and Y. Zhang

*Department of Physics and Astronomy, Dartmouth College, Hanover, NH 03755*

(Dated: September 14, 2018)

We analyze the dynamics of a nano-mechanical resonator coupled to a single-electron transistor (SET) in the regime where the resonator behaves classically. A master equation is derived describing the dynamics of the coupled system which is then used to obtain equations of motion for the average charge state of the SET and the average position of the resonator. We show that the action of the SET on the resonator is very similar to that of a thermal bath, as it leads to a steady-state probability-distribution for the resonator which can be described by mean values of the resonator position, a renormalized frequency, an effective temperature and an intrinsic damping constant. Including the effects of extrinsic damping and finite temperature, we find that there remain experimentally accessible regimes where the intrinsic damping of the resonator still dominates its behavior. We also obtain the average current through the SET as a function of the coupling to the resonator.

## I. INTRODUCTION

Recent developments in fabrication have made it possible to produce nano-electromechanical systems in which mechanical resonators with frequencies in the range 100 MHz–1 GHz are coupled electrostatically to mesoscopic conductors.<sup>1,2,3,4,5,6,7</sup> The dynamics of nano-electromechanical systems have attracted considerable interest because of the novel transport mechanisms they can give rise to,<sup>8,9,10,11</sup> their interesting non-linear and chaotic properties<sup>3,12,13</sup> and their applications as fast and ultra-sensitive sensors.<sup>2,4</sup> Furthermore, when cooled to ultra-low temperatures, high-frequency resonators are expected to display quantum mechanical behavior and so nano-electromechanical devices could be used to explore the cross-over from quantum to classical behavior in mechanical systems.<sup>14,15,16,17</sup>

Theoretical,<sup>18,19,20</sup> and experimental,<sup>7</sup> work has suggested that a single-electron transistor (SET) could form the basis of an extremely sensitive motion detector for nano-mechanical resonators. Therefore, the question of what the potential sensitivity of such a displacement detector will be, and how it is determined by the underlying dynamics of the coupled SET–resonator system, is of practical as well as theoretical interest.

When a mechanical resonator, coated with a thin metallic layer, is placed next to a SET, it acts like a capacitor whose presence affects the current flowing through the SET. The capacitance, and therefore the current, depend on the position and hence the motion of the resonator. The sensitivity with which the displacement of a resonator can be measured from the current through the SET is limited by two sources of noise. Firstly, the shot noise in the current through the SET limits its sensitivity. Secondly, the fluctuating charge on the SET island will act as a fluctuating force on the resonator, resulting ultimately in displacement noise. Thus far, the sensitivity of the displacement detection which can be achieved has been gauged by treating the resonator and the SET as two distinct elements.<sup>20</sup> Although this approach provides a reasonably accurate estimate of the sensitivity, it neglects correlations between the displacement noise of the resonator and the shot noise in the current. In fact, the coupled SET and resonator form an intrinsically interesting dynamical system in their own right. By studying the full coupled dynamics of the system a broad understanding of the underlying physics can be achieved which can then be applied to obtain important insights into when the system would function most sensitively as a measuring device.

In this article, we analyze the coupled dynamics of the SET–resonator system, treating the resonator as a classical harmonic oscillator. In particular, we examine the effect on the motion of the resonator of electrons tunnelling through the SET and the concomitant effects of the resonator motion on the average current of the SET. More generally, our analysis of the coupled dynamics provides useful insights into the dynamical behavior of nano-electromechanical systems.

The dynamics of a *quantum* harmonic oscillator coupled to an electrical tunnel junction was studied recently by Mozyrsky and Martin<sup>17</sup> and by Smirnov *et al.*<sup>22</sup> In the regime where the drain-source voltage across the junction,  $V_{ds}$ , is much larger than the energy quanta of the oscillator,  $\hbar\omega_0$ , Mozyrsky and Martin found that the dynamics of the density matrix of the oscillator reduced to a form very similar to that of the Caldeira–Leggett model<sup>23</sup> for an oscillator in contact with a thermal bath. From the connection with the Caldeira–Leggett model, Mozyrsky and Martin were able to show that the tunnelling electrons caused rapid dephasing of the oscillator, acting like a thermal

bath with an effective temperature and associated damping constant.

For a classical resonator coupled only to a SET, we find that the electrons affect the resonator in a similar way to the quantum system considered by Mozyrsky and Martin.<sup>17</sup> For sufficiently weak coupling between the resonator and the SET, the electrons act like a thermal bath which heats the resonator to an effective temperature. However, if the coupling between the SET and the resonator is increased the behavior of the resonator begins to deviate significantly from that of an oscillator in contact with a thermal bath. Including the effects of extrinsic damping of the resonator, we find that the effective temperature of the resonator is suppressed.

The classical regime for the resonator which we consider here will be the appropriate description for systems where  $eV_{ds} \gg \hbar\omega_0$  and the model we use to treat the electron tunnelling processes in the SET will require  $eV_{ds} \gg k_B T_e$ ,<sup>24</sup> where  $T_e$  is the electron temperature (assumed to be the same in the SET island and leads). As the electrons passing through the SET heat the resonator to an effective temperature which is proportional to  $eV_{ds}$  in the absence of extrinsic damping, this means that the resonator effective temperature can be much larger than the electron temperature. We will assume possible overheating of the SET can be neglected,<sup>25,26</sup> so that this temperature imbalance can be maintained and the above model assumptions continue to hold.

The outline of this paper is as follows. In Sec. II, we review the properties of the SET with a fixed voltage gate and the master equation method which can be used to determine the average current. Then in Sec. III, we generalize the results for a fixed voltage gate to the case where the gate is a nano-mechanical resonator. Initially, we analyze the dynamics of the resonator coupled to the SET ignoring external influences. We derive the equations of motion for the probability distribution of the system and show that, with certain approximations, the average properties of the system can be described by simple, physically intuitive equations of motion. We investigate the steady-state properties of the probability distribution for the coupled system by numerical integration of the master equations that govern the dynamics.

In Sec. IV, we consider the effect of damping in the resonator, arising from sources other than the interaction with the SET, and the effect of finite background temperature. We examine the current characteristics of the system in Sec. V, and obtain the average current through the SET when it is coupled to the resonator. Then in Sec. VI, we discuss how our results could be investigated experimentally. Finally, in Sec. VII, we draw our conclusions and discuss the more general implications of our results for understanding the dynamics of nano-electromechanical systems.

In the appendices we give further details about aspects of our calculations. In appendix A, we derive the Hamiltonians and electron tunnelling rates for the coupled SET–resonator system. We give details of the method used to integrate the master equations for the SET–resonator probability distribution in appendix B. The effect of higher vibrational modes of the nano-mechanical resonator is discussed in appendix C. Finally, in appendix D we estimate the typical experimentally achievable values of the parameters appearing in our model.

## II. CHARGE DYNAMICS OF A SET COUPLED TO A FIXED GATE

The development of the single-electron transistor (SET)<sup>27</sup> and its subsequent refinement<sup>28</sup> offers the prospect of carrying out electrometry with unprecedented accuracy.<sup>29</sup> A SET consists of a small metal island joined to leads by two tunnel junctions. The small capacitance of the metal island can give rise to a Coulomb blockade where the charging energy of a single electron dominates over thermal effects at low temperatures and the only accessible state of the system has a fixed number of electrons on the island,  $N$ . An external voltage-gate can be used to induce a polarization charge on the metal island which makes the states with  $N$  and  $N + 1$  electrons degenerate, and thus allows current to flow through the device. In the low temperature regime, states with more than  $N + 1$  or fewer than  $N$  electrons have much higher energies because of charging effects and so play no role in the dynamics of the system.<sup>30</sup>

Before we go on to consider the coupled dynamics of the SET-resonator system, we briefly review the properties of the SET when coupled to a fixed voltage-gate. The circuit diagram for a nano-mechanical resonator coupled to the island of a single-electron transistor is shown schematically in Fig. 1. Neglecting the effect of the dynamics, the resonator acts as a simple voltage-gate with a fixed position. Indeed, the dynamics of the resonator, which we consider in the next section, generally acts as a small perturbation on top of the effect of a static voltage gate.

We simplify the analysis a little by assuming that the SET is symmetrical, as shown in Fig. 1. The two junctions linking the metal island to the leads have the same capacitances,  $C_j$ , resistances,  $R$ , and a drain-source voltage  $V_{ds}$  (which we take to be positive throughout) is applied across the island symmetrically. The static resonator acts as the gate of a capacitor,  $C_g$ , with a voltage  $V_g$  applied to it. The gate voltage can have a strong influence on the charge dynamics of the electrons on the island because of the polarization charge it induces.

The energy of  $N$  charges on the SET island with a fixed gate is given, up to an unimportant constant factor, by<sup>31</sup>

$$H_N = \frac{e^2}{2C_\Sigma} (N^2 - 2NN_g), \quad (1)$$

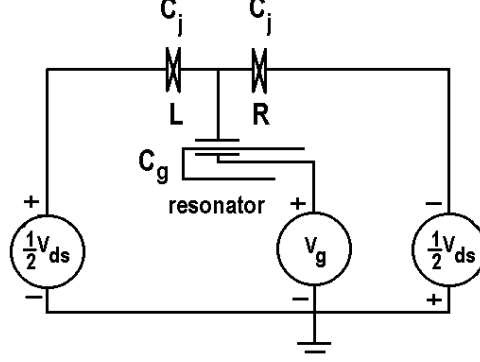


FIG. 1: Circuit diagram for the coupled SET-resonator system. The SET island lies between the two tunnel junctions which are assumed to have the same capacitance  $C_j$ . Under the drain-source voltage shown, the electrons tend to flow through the SET island from right to left.

where  $C_\Sigma = 2C_j + C_g$  is the total capacitance of the SET, and  $N_g = -C_g V_g / e$  is the polarization charge induced by the gate.

In the regime where  $e^2 / (2C_\Sigma) \gg k_B T_e$ , and where the bias voltage is not too large, the electron tunnelling processes in the SET are restricted to those between  $N$  and  $N + 1$  electrons on the island.<sup>19,20,31</sup> The tunnelling dynamics of the electrons can be modelled by a simple master equation known as the orthodox model.<sup>30</sup> This approach is valid provided that the effective tunnel junction resistances satisfy  $R > h/e^2$ , the charging energy dominates over the thermal energy, and the SET is biased well away from the Coulomb blockade regions so that co-tunnelling can be neglected.

We now outline the form of the master equation and the way in which the steady-state current is obtained for the SET with a fixed gate. The analysis of the coupled dynamics of the SET-resonator system is then carried out by generalizing these results to include the motion of the resonator.

### A. Master Equation

Within the orthodox model,<sup>30</sup> the state of an ensemble of SETs for which only the two charge states  $N$  and  $N + 1$  are accessible can be described by the probabilities  $P_N(t)$  and  $P_{N+1}(t)$ , of finding  $N$  or  $N + 1$  electrons on the island at time  $t$ , respectively. These probabilities evolve in time according to a pair of coupled master equations,

$$\frac{dP_N}{dt} = -(\Gamma_L^- + \Gamma_R^+)P_N + (\Gamma_L^+ + \Gamma_R^-)P_{N+1} \quad (2)$$

$$\frac{dP_{N+1}}{dt} = (\Gamma_L^- + \Gamma_R^+)P_N - (\Gamma_L^+ + \Gamma_R^-)P_{N+1}, \quad (3)$$

where  $\Gamma_{L(R)}^\pm$  are the tunnelling rates forwards (+) or backwards (-) across the two junctions  $L$  and  $R$  between the island and the leads, as illustrated in Fig. 1. Here we use the convention that the forward direction is from right to left, matching the direction set by the drain-source voltage. The tunnelling rates are calculated using the orthodox model and at finite temperature,  $T_e$ , are given by<sup>30</sup>

$$\Gamma_{L(R)}^\pm = \frac{1}{e^2 R} \frac{\Delta E_{L(R)}^\pm}{1 - e^{-\Delta E_{L(R)}^\pm / k_B T_e}}, \quad (4)$$

where  $\Delta E_{L(R)}^\pm$  is the initial free energy (of the SET and leads) before tunnelling through the  $L(R)$  junction, minus the final free energy after tunnelling forwards (+) or backwards (-). At  $T_e = 0$ , this expression reduces to the simplified form,

$$\Gamma^\pm = \frac{1}{e^2 R} \Delta E_{L(R)}^\pm \Theta(\Delta E_{L(R)}^\pm), \quad (5)$$

where  $\Theta(x)$  is the Heaviside step-function.

### B. SET Current

The current through the SET depends on the tunnelling rates through the two junctions. In the steady-state, current conservation means that we need only ever consider electron tunnelling processes across one junction. When the Coulomb-blockade limits the accessible charge states of the SET island to  $N$  and  $N + 1$ , the steady-state current can be written as<sup>32</sup>

$$\langle I \rangle = e (\Gamma_L^+ P_{N+1} - \Gamma_L^- P_N) \quad (6)$$

$$= e (\Gamma_R^+ P_N - \Gamma_R^- P_{N+1}), \quad (7)$$

where  $\langle \dots \rangle$  denotes an ensemble average and where  $P_N$  and  $P_{N+1} = 1 - P_N$  are the probabilities of having  $N$  and  $N + 1$  electrons on the island, respectively. Substituting in the correct expressions for the tunnelling rates, we find

$$\langle I \rangle = \frac{e}{\tau_t} P_N P_{N+1}, \quad (8)$$

where  $\tau_t = Re/V_{ds}$  is a measure of the average time between tunnelling events.

## III. DYNAMICS OF THE COUPLED SET AND RESONATOR

Unlike a fixed voltage-gate, a movable voltage-gate, such as a nano-mechanical resonator, responds dynamically to the force exerted on it by electrons tunnelling through the SET island. Furthermore, the motion of the resonator acts back on the SET by altering the tunnelling rates of the electrons. The coupled dynamics of the SET electrons and the resonator eventually results in a steady-state, even without including the effects of external sources of dissipation on the resonator.

The dynamics of the SET-resonator system are described by generalizing the master equation for the SET charges to include the position and velocity of the resonator. Crucially, the tunnelling rates for electrons in the master equation must be re-calculated to include the effect of the resonator's motion. Although the master equation for the SET-resonator system is apparently much more complicated than that for the fixed-gate case, the dynamics of the average resonator position and SET charge are readily determined once certain simplifying approximations are made. Furthermore, the master equation can be solved numerically and it is found that for sufficiently weak coupling the steady-state probability distributions are approximately Gaussian in form. The effect of the SET on the motion of the resonator can then be gauged very accurately from the first and second moments of the steady-state probability distribution.

We treat the nano-mechanical resonator as a single-mode harmonic oscillator, as it turns out that the interaction between the SET and the fundamental flexural mode of the resonator dominates the behavior. However, if we assume that interactions between the various vibrational modes of the nano-mechanical resonator can be neglected, then the results we obtain for a single mode can be generalized to include higher frequency modes.

### A. Master Equation

The probability distribution for the SET-resonator system is a function of the oscillator position,  $x$ , and velocity,  $u$ , as well as the charge state of the SET island. We can characterize the state of the system by the probability distribution pair,  $P_N(x, u; t)$  and  $P_{N+1}(x, u; t)$ , which give the probabilities of the oscillator being at position  $x$ , with velocity  $u$ , and having  $N$  or  $N + 1$  electrons on the island, respectively, at time  $t$ . At  $T_e = 0$ , the equations of motion for these probability distributions take the form,

$$\begin{aligned} \frac{dP_N(x, u; t)}{dt} = & \{H_N, P_N(x, u; t)\} \\ & + \frac{1}{Re^2} [\Theta(\Delta E_L^+) \Delta E_L^+ + \Theta(\Delta E_R^-) \Delta E_R^-] P_{N+1}(x, u; t) \\ & - \frac{1}{Re^2} [\Theta(\Delta E_R^+) \Delta E_R^+ + \Theta(\Delta E_L^-) \Delta E_L^-] P_N(x, u; t) \end{aligned} \quad (9)$$

$$\begin{aligned} \frac{dP_{N+1}(x, u; t)}{dt} = & \{H_{N+1}, P_{N+1}(x, u; t)\} \\ & + \frac{1}{Re^2} [\Theta(\Delta E_R^+) \Delta E_R^+ + \Theta(\Delta E_L^-) \Delta E_L^-] P_N(x, u; t) \\ & - \frac{1}{Re^2} [\Theta(\Delta E_L^+) \Delta E_L^+ + \Theta(\Delta E_R^-) \Delta E_R^-] P_{N+1}(x, u; t), \end{aligned} \quad (10)$$

where  $H_{N(N+1)}$  is the Hamiltonian for the SET-resonator system with  $N(N+1)$  electrons on the island, and  $\{\cdot, \cdot\}$  is a Poisson bracket. The quantities  $\Delta E_{L(R)}^\pm$  are the total free energy differences for an electron tunnelling forwards (+) or backwards (-) across the left-hand (right-hand) junction.

The Hamiltonians for the coupled SET-resonator system with  $N$  and  $N+1$  electrons on the SET island are readily obtained treating the resonator as a single-mode harmonic oscillator, with angular frequency  $\omega_0$ , centered a distance  $d$  away from the SET island. Details of the calculation are given in appendix A. The Hamiltonians take the form

$$H_N = E_c \delta N + \frac{p^2}{2m} + \frac{1}{2} m \omega_0^2 x^2 \quad (11)$$

$$H_{N+1} = -E_c \delta N + \frac{p^2}{2m} + \frac{1}{2} m \omega_0^2 (x - x_0)^2 - \frac{1}{2} m \omega_0^2 x_0^2 \quad (12)$$

$$-m \omega_0^2 x_0^2 (N_g - \delta N - 1/2), \quad (13)$$

where  $\delta N = N_g - N - 1/2$  and  $x_0 = -2E_c N_g / (m \omega_0^2 d)$ . The length-scale  $x_0$  has a simple physical interpretation: it is the distance between the equilibrium positions for the resonator with  $N$  and  $N+1$  electrons on the SET island.

The energy differences which determine the tunnelling rates are given by

$$\Delta E_L^+ = -\Delta E_L^- = -2E_c \delta N - m \omega_0^2 x_0 x - m \omega_0^2 x_0^2 (N_g - \delta N - 1/2) + \frac{eV_{ds}}{2} \quad (14)$$

$$\Delta E_R^+ = -\Delta E_R^- = 2E_c \delta N + m \omega_0^2 x_0 x + m \omega_0^2 x_0^2 (N_g - \delta N - 1/2) + \frac{eV_{ds}}{2}, \quad (15)$$

as derived in appendix A. Notice that at  $T_e = 0$ , for a given displacement of the resonator and voltage bias, tunnelling across each junction will only be able to occur in one direction. The equations of motion for the probability distributions can be extended to finite temperatures by replacing the tunnelling rates by the appropriate finite temperature form, as given in Eq. (4).

## B. Mean-Coordinate Dynamics

Integration of the coupled master equations gives a complete description of the ensemble dynamics. However, the equations of motion for the probability distribution are complicated and it is not easy to extract an overall picture of the dynamics from them. Nevertheless, by making a few physically motivated approximations, it is possible to obtain equations of motion for all of the first and second moments of the distributions.

In order to simplify the analysis, we assume that  $\delta N$ ,  $V_{ds}$ , and the range of  $x$  for which the probabilities,  $P_N(x, u; t)$  and  $P_{N+1}(x, u; t)$ , are non-negligible are such that  $\Delta E_L^+, \Delta E_R^+$  are always positive. Such an approximation is valid so long as the drain-source voltage is the dominant energy scale so that  $eV_{ds} \gg m \omega_0^2 x_0^2, E_c \delta N$  and the distributions  $P_N(x, u; t)$  and  $P_{N+1}(x, u; t)$  are strongly peaked at  $x \sim x_0$ .

Taking into account this approximation, we need only consider two out of the four tunnelling processes, as the step function constraints will always be satisfied for the processes in the ‘+’ direction, and never satisfied for processes in the ‘-’ direction. Thus, we obtain a simplified pair of coupled master equations,

$$\frac{dP_N}{dt} = \omega_0^2 x \frac{\partial P_N}{\partial u} - u \frac{\partial P_N}{\partial x} + \frac{1}{Re^2} (E_L P_{N+1} - E_R P_N - m \omega_0^2 x_0 x P) \quad (16)$$

$$\frac{dP_{N+1}}{dt} = \omega_0^2 (x - x_0) \frac{\partial P_{N+1}}{\partial u} - u \frac{\partial P_{N+1}}{\partial x} - \frac{1}{Re^2} (E_L P_{N+1} - E_R P_N - m \omega_0^2 x_0 x P), \quad (17)$$

where  $P(x, u; t) = P_N(x, u; t) + P_{N+1}(x, u; t)$ , and we have defined  $E_L = -2E_c \delta N - m \omega_0^2 x_0^2 (N_g - \delta N - 1/2) + eV_{ds}/2$  and  $E_R = 2E_c \delta N + m \omega_0^2 x_0^2 (N_g - \delta N - 1/2) + eV_{ds}/2$  (i.e.,  $E_L$  and  $E_R$  are the position-independent parts of  $\Delta E_L^+$  and  $\Delta E_R^+$ , respectively).

Adding together Eqs. (16) and (17), the tunnelling terms cancel out and we obtain the simplified equation of motion for the full probability distribution.

$$\frac{dP}{dt} = \omega_0^2 x \frac{\partial P}{\partial u} - u \frac{\partial P}{\partial x} - x_0 \frac{\partial P_{N+1}}{\partial u}. \quad (18)$$

We can now obtain equations which describe the dynamics of the ensemble-averaged position and velocity by multiplying Eq. (18) by  $x$  and  $u$  respectively and then integrating over both  $x$  and  $u$ ,

$$\langle \dot{u}(t) \rangle = -\omega_0^2 \langle x(t) \rangle + \omega_0^2 x_0 \langle P \rangle_{N+1}(t) \quad (19)$$

$$\langle \dot{x}(t) \rangle = \langle u(t) \rangle \quad (20)$$

where the averages are defined by

$$\langle \cdots \rangle = \int dx \int du (\cdots) (P_{N+1}(x, u; t) + P_N(x, u; t))$$

and

$$\langle P \rangle_{N+1} = \int dx \int du P_{N+1}(x, u; t).$$

We can obtain a closed set of equations by integrating Eq. (17) over  $x$  and  $u$  to obtain,

$$Re^2 \langle \dot{P} \rangle_{N+1}(t) = E_R - eV_{ds} \langle P \rangle_{N+1}(t) - m\omega_0^2 x_0 \langle x(t) \rangle. \quad (21)$$

### 1. Fixed Point Analysis

The steady-state behavior of the system is described by the fixed-points of the mean-coordinate equations (19,20,21). Setting  $\langle \dot{u} \rangle = \langle \dot{x} \rangle = \langle \dot{P} \rangle_{N+1} = 0$ , we find that there is a single solution at

$$\langle u \rangle_{\text{fp}} = 0 \quad (22)$$

$$\langle x \rangle_{\text{fp}} = x_0 (\langle P \rangle_{N+1})_{\text{fp}} \quad (23)$$

$$(\langle P \rangle_{N+1})_{\text{fp}} = \frac{2E_C \delta N + m\omega_0^2 x_0^2 (N_g - \delta N - 1/2) + eV_{ds}/2}{eV_{ds} - m\omega_0^2 x_0^2}. \quad (24)$$

In order to make the physical content of the mean-coordinate equations (19,20,21) more apparent, we transform them to variables centered on their fixed points,

$$\langle \tilde{x} \rangle = \langle x \rangle - \langle x \rangle_{\text{fp}} \quad (25)$$

$$\langle \tilde{P} \rangle_{N+1} = \langle P \rangle_{N+1} - (\langle P \rangle_{N+1})_{\text{fp}}, \quad (26)$$

and we also re-express them in terms of the dimensionless frequency and coupling strength parameters  $\epsilon = \omega_0 \tau_t$  and  $\kappa = m\omega_0^2 x_0^2 / (eV_{ds})$ , respectively. Hence we find,

$$\langle \dot{\tilde{P}} \rangle_{N+1} = \frac{\kappa}{x_0} \langle \tilde{x} \rangle - \langle \tilde{P} \rangle_{N+1} \quad (27)$$

$$\langle \dot{\tilde{x}} \rangle = \langle u \rangle \quad (28)$$

$$\langle \dot{u} \rangle = \epsilon^2 (x_0 \langle \tilde{P} \rangle_{N+1} - \langle \tilde{x} \rangle). \quad (29)$$

where the time coordinate has been scaled by the tunnelling time,  $\tau_t$ .

The scaled parameter  $\epsilon$  compares the relative time-scales of the oscillator period and electron tunnelling time. Generally, the oscillator motion will be much slower than the electron tunnelling time and so we expect  $\epsilon \ll 1$  for most practical situations. The parameter  $\kappa$  is a measure of the interaction strength between the SET and the resonator in terms of the energy-scale defined by the drain-source voltage. In practice, the coupling between the resonator and the SET which can be achieved will be weak so that  $\kappa \ll 1$ , as discussed in Sec. VI.

The mean-coordinate dynamics about the fixed point is given by a set of three coupled, linear, first-order differential equations, and the stability of the fixed point can be determined from the behavior of the associated eigenvalues. Although the eigenvalues of a system of three equations can be determined analytically, the expressions obtained are algebraically rather complicated. However, the stability of the system is determined by whether or not the real part of any of the eigenvalues becomes positive, in which case the system can become unstable. A simple numerical calculation shows that the SET-resonator system is entirely stable for  $\kappa < 1$ , but for  $\kappa > 1$  it seems that our equations predict that the system becomes unstable. However, any potential instability in the motion of the resonator would clearly involve processes which lie outside the domain of our approximate description and so we cannot draw any conclusions about the overall stability of the system within the existing model.

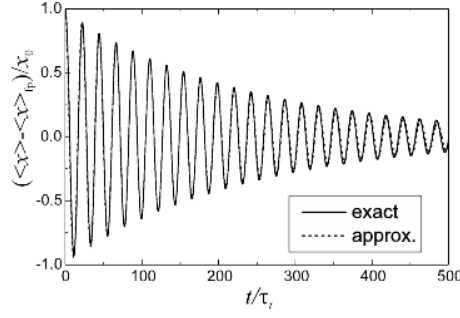


FIG. 2: Comparison of the approximate analytical equations of motion for the resonator with the exact equations, integrated numerically. In this plot  $\kappa = 0.1$  and  $\epsilon = 0.3$ , so the approximate equations are close to the limit on their validity ( $\epsilon \ll 1$ ).

## 2. Analytical Description

The set of linear equations describing the mean-coordinate dynamics of the SET-resonator system can be solved analytically, and the general solution obtained. However, as with the eigenvalues, the general solution is algebraically too complicated to be useful in developing an intuitive picture of the dynamics. However, in the regime where  $\epsilon \ll 1$  and  $\kappa < 1$  a very good approximation to the full solution can be derived as an expansion in  $\epsilon$ .

The approximate solutions for the trajectory of the system take the form,

$$\langle \tilde{x}(t) \rangle = e^{-\kappa \epsilon^2 t / 2 \tau_t} \left[ \tilde{x}(0) \cos(\sqrt{1 - \kappa} \epsilon t / \tau_t) + \frac{u(0)}{\sqrt{1 - \kappa} \epsilon} \sin(\sqrt{1 - \kappa} \epsilon t / \tau_t) \right] \quad (30)$$

$$\begin{aligned} \langle \tilde{P} \rangle_{N+1}(t) &= \left( \tilde{P}_{N+1}(0) - \kappa \frac{\tilde{x}(0)}{x_0} \right) e^{-(1 - \kappa \epsilon^2) t / \tau_t} \\ &+ e^{-\kappa \epsilon^2 t / 2 \tau_t} \frac{\kappa}{x_0} \left[ \tilde{x}(0) \cos(\sqrt{1 - \kappa} \epsilon t / \tau_t) + \frac{u(0)}{\sqrt{1 - \kappa} \epsilon} \sin(\sqrt{1 - \kappa} \epsilon t / \tau_t) \right] \end{aligned} \quad (31)$$

with the initial conditions  $\langle \tilde{x}(t=0) \rangle = \tilde{x}(0)$ ,  $\langle u(t=0) \rangle = u(0)$  and  $\langle \tilde{P}_{N+1}(t=0) \rangle = \tilde{P}_{N+1}(0)$ . The approximate trajectory is in fact very close to the full solution, as is shown in Fig. 2 for  $\kappa = 0.1$  and  $\epsilon = 0.3$ . The value of  $\epsilon$  in the plot is at the limit of the range of validity of the approximate equations, but the agreement remains good. For values of  $\epsilon < 0.1$  the approximate and exact curves overlay each other so well that the two curves cannot easily be distinguished.

The approximate analytical solution for the dynamics of the oscillator given by Eq. (30) can be obtained from the equation of motion for a damped harmonic oscillator, with damping constant  $\kappa \epsilon^2 / \tau_t$ , and (angular) frequency  $\sqrt{1 - \kappa} \epsilon / \tau_t$ . The shift in frequency is due to the interaction between the oscillator and the tunnelling electrons.<sup>23</sup> We can think of  $\gamma_i = \kappa \epsilon^2 / \tau_t$  as an *intrinsic* damping rate for the SET-resonator system, to be distinguished from *extrinsic* damping arising from sources other than interaction with the SET (see subsection IV A).

## C. Numerical Solution of the Coupled Master Equations

As well as extracting mean-coordinate properties, it is possible to integrate the equations for the probability distributions [Eqs. (16) and (17)] numerically, using a method which is outlined in appendix B. Numerical integration allows us to demonstrate that the coupled master-equations do indeed lead to a steady-state probability distribution and also to explore how this steady-state is reached.

Figure 3 shows the dynamics of the variance,  $\delta x^2$ , of the full probability distribution,  $P(x, u; t)$ . The initial probability distributions were chosen to be sharply peaked in phase space. For simplicity we have performed all the calculations at a gate-voltage such that  $E_L = E_R = eV_{ds}/2$ , so that the  $N$  and  $N + 1$  charge states would be degenerate in the limit  $\kappa = 0$ . After some initial oscillations,  $\delta x^2$  settles down to a steady value. The rate at which the steady-state is achieved is  $\gamma_i$ , just as we would expect for a damped harmonic oscillator. Notice, however, that all the lengths have been scaled by  $x_0$ , which itself depends on  $\kappa$ . Thus, the absolute magnitude of the variances increase with  $\kappa$  in contrast to the scaled values which actually decrease.

The steady-state probability distributions  $P(x)$ , for  $\epsilon = 0.3$  and  $\kappa = 0.1, 0.05$ , and  $0.01$ , respectively, are shown in comparison with the appropriate Gaussian fits in Fig. 4. The steady-state distributions are indeed strongly peaked,

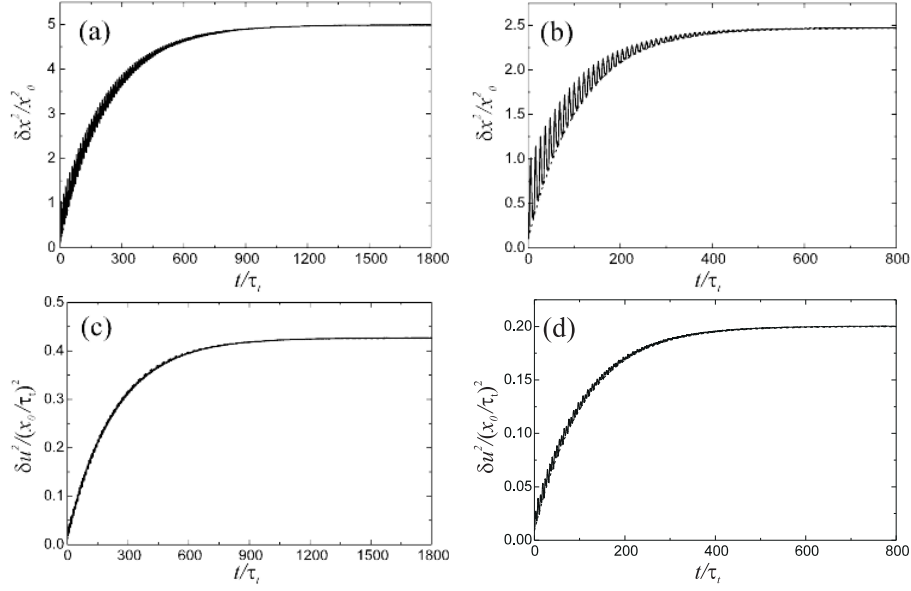


FIG. 3: Behavior of the variances,  $\delta x^2$  and  $\delta u^2$ , as the steady-state is approached. In panels (a) and (c)  $\kappa = 0.05$ , and in panels (b) and (d)  $\kappa = 0.1$ , with  $\epsilon = 0.3$  throughout. The dashed lines represent fits to an exponential time-dependence obtained using the initial variances, the steady-state values calculated using Eqs. (42) and (43), and the appropriate decay rate,  $\gamma_i = \epsilon^2 \kappa$ , in each case.

as we assumed earlier, and the overall distribution is very nearly Gaussian as can be seen from the plots which are generated from the average position and associated variance in each case. The deviation from a Gaussian distribution is most apparent for  $\kappa = 0.1$  and the agreement improves as the coupling is reduced. The sub-distributions  $P_N(x)$  and  $P_{N+1}(x)$  for  $\kappa = 0.1$  are shown in Fig. 4(d). They are clearly centered on different points and also closely resemble Gaussians individually. However, since one cannot add two displaced Gaussians to obtain a single Gaussian curve, it is clear that the curves are not exactly Gaussian in form.

#### D. Variances of the distribution

Since the steady-state distribution is close to Gaussian for  $\kappa \ll 1$ , the state of the resonator in this regime will be almost completely specified by the average values of its coordinates and their variances. Making use of the fact that there is indeed a well-defined steady-state, we can derive analytical expressions for the variances in the resonator position and velocity.

Multiplying Eqs. (16,17) by the appropriate quantity and integrating over the position and velocity of the resonator, we obtain the following closed set of equations of motion:

$$\langle \dot{x}u \rangle = -\omega_0^2 \langle x^2 \rangle + \langle u^2 \rangle + \omega_0^2 x_0 \langle x \rangle_{N+1} \quad (32)$$

$$\langle \dot{x}^2 \rangle = 2 \langle xu \rangle \quad (33)$$

$$\langle \dot{u}^2 \rangle = -2\omega_0^2 \langle xu \rangle + 2x_0\omega_0^2 \langle u \rangle_{N+1} \quad (34)$$

$$\langle \dot{x} \rangle_N = \langle u \rangle_N + \frac{1}{Re^2} [E_L \langle x \rangle_{N+1} - E_R \langle x \rangle_N - m\omega_0^2 x_0 \langle x^2 \rangle] \quad (35)$$

$$\langle \dot{x} \rangle_{N+1} = \langle u \rangle_{N+1} - \frac{1}{Re^2} [E_L \langle x \rangle_{N+1} - E_R \langle x \rangle_N - m\omega_0^2 x_0 \langle x^2 \rangle] \quad (36)$$

$$\langle \dot{u} \rangle_N = -\omega_0^2 \langle x \rangle_N + \frac{1}{Re^2} [E_L \langle u \rangle_{N+1} - E_R \langle u \rangle_N - m\omega_0^2 x_0 \langle ux \rangle] \quad (37)$$

$$\langle \dot{u} \rangle_{N+1} = -\omega_0^2 \langle x \rangle_{N+1} + \omega_0^2 x_0 \langle P \rangle_{N+1} - \frac{1}{Re^2} [E_L \langle u \rangle_{N+1} - E_R \langle u \rangle_N - m\omega_0^2 x_0 \langle ux \rangle], \quad (38)$$

where  $\langle \dots \rangle_N$  and  $\langle \dots \rangle_{N+1}$  imply averages over the sub-distributions  $P_N(x, u)$  and  $P_{N+1}(x, u)$ , respectively.

In the steady-state, all time derivatives will be zero and hence we can infer the following properties of the stationary

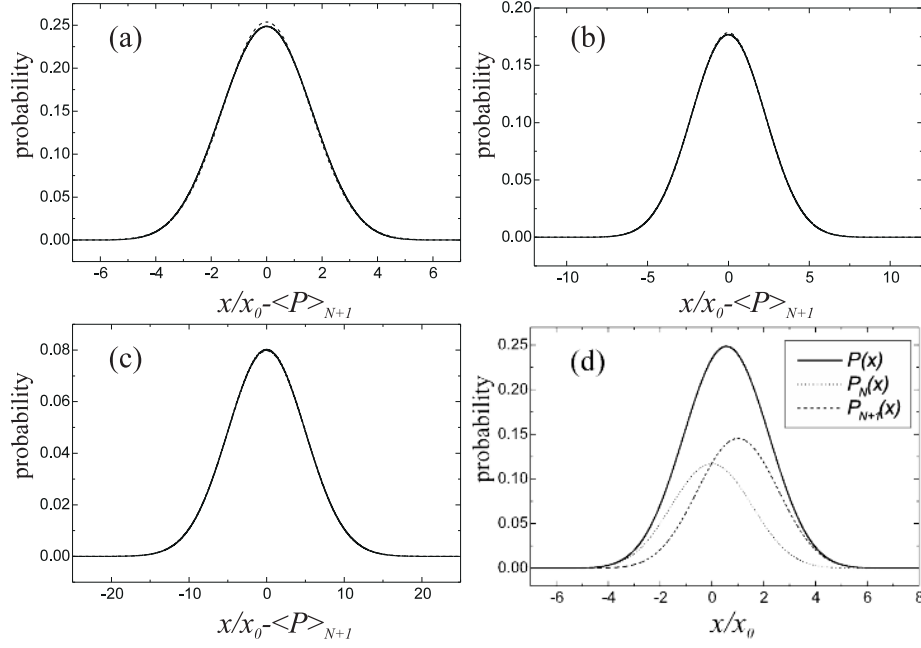


FIG. 4: Steady-state probability distributions as a function of position. The full probability distribution,  $P(x)$ , centered on the fixed point  $x_0\langle P\rangle_{N+1}$ , is shown in (a) with  $\kappa = 0.1$ , (b) with  $\kappa = 0.05$ , and (c) with  $\kappa = 0.01$ , where  $\epsilon = 0.3$  in each case. Each of the numerical curves is compared with a Gaussian fitted using the fixed-point position and the position variance, obtained from Eqs. (23) and (42) respectively. In (d) the sub-distributions  $P_N(x)$  and  $P_{N+1}(x)$  for  $\kappa = 0.1$  and  $\epsilon = 0.3$  are shown.

distribution

$$\langle x \rangle_{N+1} = x_0 \langle P \rangle_{N+1} \quad (39)$$

$$\langle u^2 \rangle - \omega_0^2 \langle x^2 \rangle = -\omega_0^2 x_0 \langle x \rangle_{N+1} \quad (40)$$

$$\langle x^2 \rangle = \frac{E_L}{m\omega_0^2} \langle P \rangle_{N+1}, \quad (41)$$

and  $\langle xu \rangle = \langle u \rangle_N = \langle x \rangle_N = \langle u \rangle_{N+1} = 0$ . Taken together with the steady-state solutions of the mean-coordinate equations,  $\langle x \rangle = x_0 \langle P \rangle_{N+1}$  and  $\langle u \rangle = 0$ , we obtain expressions for the variances in position and velocity for the stationary probability distribution. Thus we find,

$$\delta x^2 = \frac{x_0^2}{\kappa} \langle P \rangle_N \langle P \rangle_{N+1} = \frac{eV_{ds}}{m\omega_0^2} \langle P \rangle_N \langle P \rangle_{N+1} \quad (42)$$

$$\delta u^2 = \frac{x_0^2 \omega_0^2}{\kappa} (1 - \kappa) \langle P \rangle_N \langle P \rangle_{N+1} = \frac{eV_{ds}}{m} (1 - \kappa) \langle P \rangle_N \langle P \rangle_{N+1}. \quad (43)$$

The accuracy of these expressions, based on the assumption that only forward electron tunnelling occurs, can be tested by comparing them with the results obtained from numerical integration of the master equation. Fig. 5 compares the analytical result, Eq. (42), with the numerical result as a function of  $\kappa$ . It is clear that there is excellent agreement for  $\kappa \leq 0.1$ , but for larger values of  $\kappa$  the validity of the analytical expression breaks down.

In order to understand the expressions for the variances, Eqs. (42) and (43), we can compare them with those for a damped harmonic resonator in contact with a heat bath.<sup>33</sup> For an oscillator in contact with a bath at temperature  $T$ , we have equipartition of energy:  $m\omega_0^2 \delta x^2 = m\delta u^2 = k_B T$ . Comparison with Eqs. (42) and (43) shows that for  $\kappa \ll 1$  the steady-state probability distribution for the resonator is very close to a thermal one, and we can identify an effective temperature,  $T_{\text{eff}}$ , by analogy with the thermal case,

$$k_B T_{\text{eff}} = eV_{ds} \langle P \rangle_N \langle P \rangle_{N+1}. \quad (44)$$

The electrons passing through the SET give rise to a fluctuating force on the oscillator as its equilibrium position is shifted back and forth by  $x_0$ , but because the oscillator acts back on the motion of the electrons through the tunnelling rate, the motion of the oscillator is also damped and a steady-state is achieved. For  $\kappa \ll 1$ , the steady-state is very

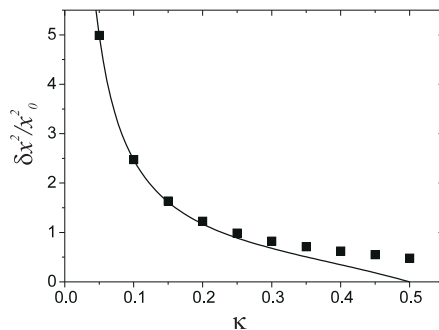


FIG. 5: Comparison of the variance,  $\delta x^2$ , calculated using Eq. (42) (curve), and the results of a numerical integration (points). Both calculations are performed for  $E_L = E_R$ .

close to a thermal state with an effective temperature which depends on properties of the SET alone: the drain-source voltage applied across it and the average probability of finding  $N$  or  $N + 1$  electrons on the island. In particular, the effective temperature does not seem to depend at all on the strength of the coupling between the resonator and the SET. In fact, the strength of the coupling  $\kappa$  does affect the effective temperature, as the values of  $\langle P \rangle_{N+1}$  and  $\langle P \rangle_N$  depend (albeit weakly) on  $\kappa$  for  $\kappa \ll 1$ . However, the value of the damping constant,  $\gamma_i$ , is proportional to  $\kappa$ , and so the coupling strength controls how long it takes for the steady state to be reached. If the coupling between the SET and the resonator is switched off (i.e.,  $\kappa = 0$ ), then Eqs. (42) and (43) break down because a steady-state for the resonator is never achieved as there is no damping.

It is interesting to compare the expressions for the effective temperature and damping constant of the resonator with results for a quantum oscillator coupled to a single electrical tunnel junction (TJ).<sup>17,22</sup> Our results for a classical oscillator can be compared directly with calculations for a quantum oscillator when  $eV_{ds} \gg \hbar\omega_0$  so that the electrons cause rapid dephasing of the resonator and induce the transition from quantum to classical behavior.<sup>17</sup> The effective temperature we obtain for a resonator coupled to a SET [Eq. (44)] is very similar to that obtained for a resonator coupled to a TJ,  $k_B T_{\text{eff}} = eV_{ds}/2$  (with the electron temperature set to zero in the electrodes). However, because  $\langle P \rangle_N \langle P \rangle_{N+1} \leq 1/4$ , the heating induced by the SET will always be at least a factor of  $1/2$  less than that induced by the TJ. In fact, the effective temperatures obtained for both the TJ and SET can be commonly equated to one-half the ensemble-averaged energy dissipated by an electron due to tunnelling across a junction. For the TJ, the energy dissipated (for zero electron temperature in the electrodes) is always  $eV_{ds}$ . For the SET, on the other hand, the average energy dissipated by a tunnelling electron is  $E_R \langle P \rangle_N + E_L \langle P \rangle_{N+1} = 2E_L \langle P \rangle_{N+1} \simeq 2eV_{ds} \langle P \rangle_N \langle P \rangle_{N+1}$  for  $\kappa \ll 1$ .

The intrinsic damping constant for the TJ takes the form  $\gamma_{\text{TJ}} = \mu C^2/m$ , to lowest order in the coupling constant  $C$ , where  $\mu$  is a constant which depends on the densities of states in the leads. In contrast, for the SET the intrinsic damping rate,  $\gamma_i = (Re^3/md^2)(V_g C_g/v_{ds} C_\Sigma)^2$ , depends explicitly on the drain-source voltage. The difference in damping rates relates directly to the difference in electron tunnelling rates for a TJ and SET: for the TJ the electron tunnelling rates across the junction do not depend on the drain-source voltage, to lowest order, whereas for the SET the tunnelling rates always depend on the drain-source voltage in the orthodox regime.

#### IV. RESONATOR WITH EXTRINSIC DAMPING AND AT FINITE TEMPERATURE

Thus far, we have considered the nano-mechanical resonator and the SET as a closed system without including any external influences. Under these circumstances, and for sufficiently weak coupling to the resonator, the SET acts like a thermal reservoir which heats the oscillator and also gives rise to damping. The effective temperature in the steady-state is not a function of the coupling strength between the SET and the resonator,  $\kappa$ , but the time taken to reach that steady-state does depend on the intrinsic damping rate which in turn depends on  $\kappa$ . However, the resonator will have a finite quality-factor, even in the absence of the SET,<sup>34</sup> and if the value of the associated damping rate,  $\gamma_e$ , is much larger than that due to the SET, then it will be essential to include these damping processes in the dynamics. Furthermore, both the resonator and the electrons will be at finite temperatures, set by their surroundings (which need not necessarily be the same). The effects of extrinsic damping and finite background temperature can be taken into account by modifying the master equation formalism we have developed so far.

### A. Variances with Extrinsic Damping

The equation of motion for the probability distribution is readily modified to include extrinsic damping of a harmonic oscillator arising from sources other than its interaction with the SET. We can obtain the correct form for the coupled master equations by adding the term

$$\frac{\partial}{\partial u} (\gamma_e u P_{N(N+1)})$$

to Eqs. (16) and (17), where the extrinsic damping is modelled as a force on the oscillator of the form  $-\gamma_e u$ .<sup>33</sup>

The mean-coordinate equations (19,20,21) and the position of the fixed-point corresponding to the steady-state are unaffected by the extrinsic damping. However, this apparent lack of change belies a significant increase in the complexity of the underlying dynamics. With finite extrinsic damping, the steady-state values of  $\langle x \rangle_N$  and  $\langle x \rangle_{N+1}$  start to converge so that  $\langle x \rangle_N > 0$  and  $\langle x \rangle_{N+1} < x_0 \langle P \rangle_{N+1}$ . Furthermore, with extrinsic damping although the overall average velocity remains zero in the steady-state, the average velocities for given charge states are non-zero:  $\langle u \rangle_N = -\langle u \rangle_{N+1} \neq 0$ .

The variances of the steady-state distribution including extrinsic damping are obtained using the same method as before, and we find

$$\delta x^2 = \frac{\delta x_i^2 (1 + \alpha)}{1 + \frac{\alpha}{\epsilon^2 \kappa} [(1 - \kappa)(1 + \alpha) + \epsilon^2]} \quad (45)$$

$$\delta u^2 = \frac{\delta u_i^2}{1 + \frac{\alpha}{\epsilon^2 \kappa} [(1 - \kappa)(1 + \alpha) + \epsilon^2]}, \quad (46)$$

where  $\alpha = \gamma_e \tau_t$ , and  $\delta x_i^2$  and  $\delta u_i^2$  are the intrinsic variances (no extrinsic damping) given by Eqs. (42) and (43), respectively.

In the regime where  $\kappa, \epsilon, \alpha \ll 1$ , the effect of the SET on the resonator will depend very sensitively on the ratio  $\gamma_e/\gamma_i = \alpha/(\epsilon^2 \kappa)$ . When  $\gamma_e \ll \gamma_i$  the extrinsic damping will not cause any serious modification of the resonator's behavior. In contrast, when  $\gamma_e \gg \gamma_i$  the extrinsic damping will round-off the driving effect of the SET and we find,

$$\begin{aligned} \delta x^2 &\simeq \delta x_i^2 \frac{\gamma_i}{\gamma_e} \\ \delta u^2 &\simeq \delta u_i^2 \frac{\gamma_i}{\gamma_e} \end{aligned}$$

and

$$k_B T_{\text{eff}} \simeq \frac{\gamma_i}{\gamma_e} e V_{\text{ds}} \langle P \rangle_N \langle P \rangle_{N+1}. \quad (47)$$

These expressions are consistent with the average back-action displacement noise derived in Ref. [20].

The relative value of the intrinsic and extrinsic damping constants are also important for understanding why a single-mode description of the resonator is sufficient. It turns out that the magnitude of the intrinsic damping constant is very much larger for the fundamental flexural mode of a resonator than for higher modes. It is for this reason that the behavior of the system is dominated by the fundamental mode and our single-mode treatment is appropriate, as we discuss in appendix C.

### B. Finite Oscillator Temperature

The electrons in the SET and the resonator will be in contact with environmental degrees of freedom which will act as thermal reservoirs at finite temperature, but for the mesoscopic system we are considering, these temperatures will not necessarily be the same and their effect on the dynamics may be very different. The effect of the finite electron temperature,  $T_e$ , will be to round out the tunnelling rates and thereby change the charge dynamics of the SET somewhat. However, from the full expression for electron tunnelling rate, Eq. (4), we can see that this effect will be small so long as  $k_B T_e \ll e V_{\text{ds}}$ .

The effect of a non-zero external bath temperature for the resonator,  $T_r$ , can be gauged by adding in one further term to the coupled master equations, (16) and (17), describing diffusion in velocity space. Thus in this case the extra terms take the form,

$$\frac{\partial}{\partial u} (\gamma_e u P_{N(N+1)}) + \frac{\partial}{\partial u} \left( \frac{G}{2m^2} \frac{\partial P_{N(N+1)}}{\partial u} \right),$$

so that without the coupling to the SET, the equation of motion for the resonator probability distribution is simply Kramer's equation.<sup>33</sup> For systems close to equilibrium,  $G$  is a constant related to the background temperature by

$$G = 2mk_B T_r \gamma_e. \quad (48)$$

In the regime where  $\alpha, \epsilon, \kappa \ll 1$  we can approximate the full equations for the variances by two the expressions

$$\delta x^2 \simeq \frac{1}{m\omega_0^2} \left[ \frac{eV_{ds}\langle P \rangle_N \langle P \rangle_{N+1}}{1 + \gamma_e/\gamma_i} + \frac{k_B T_r}{1 + \gamma_i/\gamma_e} \right] \quad (49)$$

$$\delta u^2 \simeq \frac{1}{m} \left[ \frac{eV_{ds}\langle P \rangle_N \langle P \rangle_{N+1}(1 - \kappa)}{1 + \gamma_e/\gamma_i} + \frac{k_B T_r}{1 + \gamma_i/\gamma_e} \right]. \quad (50)$$

The derivation of these relations rests on the use of the fluctuation-dissipation theorem [Eq. (48)], whose validity for the non-equilibrium SET-resonator system we have assumed without proof. Nevertheless, the resulting expressions for the variances have a very intuitive form. For  $\kappa \ll 1$ , the effective oscillator temperature satisfies

$$\frac{T_{\text{eff}}}{Q_{\text{eff}}} = \frac{T_r}{Q_e} + \frac{T_i}{Q_i}, \quad (51)$$

where the extrinsic, intrinsic, and effective quality factors are defined as  $Q_e = \omega_0/\gamma_e$ ,  $Q_i = \omega_0/\gamma_i = 1/(\kappa\epsilon)$ , and  $Q_{\text{eff}}^{-1} = Q_e^{-1} + Q_i^{-1}$ , respectively. The intrinsic temperature,  $T_i$ , is given by Eq. (44). Eq. (51) is just the steady state relation for a system in thermal contact with two reservoirs at temperatures  $T_r$  and  $T_i$ , and with the thermal conductivities of the pathways between the system and each reservoir proportional to the respective damping rates (and hence inversely proportional to the quality factors).<sup>35</sup>

The relative importance of heating due to the SET and that due to the resonator's environment is controlled by the ratios  $Q_i/Q_e$  and  $T_i/T_e$ . When  $Q_i \ll Q_e$ , we have  $T_{\text{eff}} = T_i + T_r Q_i/Q_e$ . As an example application, note that this equation predicts that it would be possible to actually cool the resonator to a temperature below  $T_r$  by coupling it to an appropriate SET such that  $T_i < T_r$ .<sup>35</sup> If, in addition to  $Q_i \ll Q_e$ , we have that  $T_i \gg T_r Q_i/Q_e$ , then the resonator hardly feels the effect of the external environment and its state is determined by the interaction with the SET electrons. In contrast, when  $Q_i \gg Q_e$ , we recover Eq. (47) provided  $T_r \ll T_i Q_e/Q_i$ . If instead  $T_r \gg T_i Q_e/Q_i$ , then the external environment dominates over the SET electrons and effectively determines the state of the resonator.

In the regime where  $Q_i \gg Q_e$ , but where the ratio  $T_i/T_e$  is arbitrary, it is possible to describe the dynamics of the SET-resonator system using a very compact and intuitive formalism. Details of such an approach, which compliments that given here, will be described elsewhere.<sup>36</sup>

## V. CURRENT CHARACTERISTICS OF THE SET

The analysis we have performed so far describes the effects of the electrons on the dynamics of the resonator. However, the electrons passing through the SET are of course influenced by the motion of the resonator and this is manifested as a change in the average current through the SET.

In the absence of extrinsic damping, and at  $T_r = T_e = 0$ , the ensemble-averaged current through the SET can be calculated from the tunnelling rates and the steady-state probability distribution function:

$$\langle I \rangle_i = e \int dx \int du \frac{\Delta E_L^+(x)}{Re^2} P_{N+1}(x, u) \quad (52)$$

$$= e \int dx \int du \frac{\Delta E_R^+(x)}{Re^2} P_N(x, u) \quad (53)$$

$$= \frac{e}{\tau_t} \langle P \rangle_N \langle P \rangle_{N+1} (1 - \kappa) \quad (54)$$

$$= \frac{m}{Re^2} \delta u_i^2. \quad (55)$$

Comparing this with the fixed gate result, Eq. (8), we see that the resonator slightly reduces the current flowing through the SET.

Including extrinsic damping, we find that the averaged current becomes

$$\langle I \rangle = \langle I \rangle_i \left( \frac{\epsilon^2(\alpha + \kappa) + \alpha(1 + \alpha)}{\epsilon^2(\alpha + \kappa) + \alpha(1 + \alpha)(1 - \kappa)} \right). \quad (56)$$

TABLE I: The resonant frequency, coupling strength and intrinsic quality factor for Si cantilevers with different lengths.

$l$ in $\mu\text{m}$	1	5	10
$f_0$ in MHz	240	9.6	2.4
$\kappa/V_g^2$ in $\text{V}^{-2}$	$3 \times 10^{-7}$	$9.8 \times 10^{-4}$	0.03
$Q_i V_g^2$ in $\text{V}^2$	$2.1 \times 10^7$	$1.7 \times 10^5$	$2.1 \times 10^4$

The average current is modified by external damping because it depends on the tunnelling rates through the individual junctions which themselves depend on the properties of the sub-ensembles through  $\langle x \rangle_N$  and  $\langle x \rangle_{N+1}$ . The external damping suppresses the motion of the resonator and this is reflected in the fact that for  $\alpha \gg \epsilon^2, \kappa \epsilon^2$  the average current is effectively reduced to that for the fixed-gate SET.

## VI. PRACTICAL CONSIDERATIONS

The predicted effect of the classical back-action of the SET on the resonator using currently available technology depends crucially on the range of values of the parameters in our model which are accessible in practice. Typical, achievable values for the individual SET and resonator parameters are discussed in detail in appendix D.

The maximum effective temperature of the resonator coupled to the SET, neglecting the effect of the extrinsic damping, is  $eV_{\text{ds}}/4k_{\text{B}}$ . Considering, for example, a typical total SET capacitance  $C_{\Sigma} = 0.5$  fF and drain-source voltage  $V_{\text{ds}} = 0.5e/C_{\Sigma} = 0.16$  mV, the maximum effective temperature is about 0.5 K. Expressed in terms of the various parameters, the dimensionless coupling strength is

$$\kappa = \left( \frac{C_g}{C_{\Sigma}} \right)^2 \frac{V_g}{V_{\text{ds}}} \frac{eV_g}{m\omega_0^2 d^2}. \quad (57)$$

Substituting in the expressions for  $C_g$ ,  $m$ , and  $\omega_0$  appropriate for, say, Si and the above values for  $C_{\Sigma}$  and  $V_{\text{ds}}$ , Eq. (57) becomes

$$\kappa = 1 \times 10^{-12} V_g^2 \frac{l^5 w}{d^4 t^3}, \quad (58)$$

where the cantilever dimensions  $l$ ,  $w$ ,  $t$ , and cantilever-island gap  $d$  are expressed in micrometers, and the gate voltage  $V_g$  is given in Volts. Similarly, the intrinsic quality factor is

$$Q_i = 1.3 \times 10^{12} \frac{1}{V_g^2} \frac{t^2 d^4}{l^3 w}, \quad (59)$$

where again the dimensions are expressed in micrometers. Note the strong dependence on the cantilever length  $l$  and gap  $d$ . As might be expected, decreasing the gap and increasing the length strengthens the coupling between the SET and resonator and reduces the quality factor. This trend can be clearly seen for the range of cantilever length examples considered in Table I. In each of the examples, the transverse cantilever dimensions are  $w = 0.25 \mu\text{m}$  and  $t = 0.2 \mu\text{m}$ , and the gap is  $d = 0.1 \mu\text{m}$ .

For micron-sized resonators, the extrinsic quality factors,  $Q_e = \omega_0/\gamma_e$ , of the fundamental modes typically lie in the range<sup>37</sup>  $\sim 10^3$ – $10^4$ , which, from the first column in Table I, will be much less than the quality factors associated with intrinsic damping even for gate voltages close to vacuum breakdown  $\sim 10$  V (see appendix E). In this regime, for the one micron long example the effective temperature will be given, to a good approximation, by  $T_{\text{eff}} = T_r + T_i Q_e/Q_i < T_r + 0.24 V_g^2$  mK. Therefore, the maximum amount the SET can add to the cantilever temperature is about 24 mK for  $V_g$  tuned to current peak maximum around the breakdown voltage = 10 V. The description of the SET back-action on the resonator in this regime coincides with the analysis given in Ref. 20. On the other hand, increasing the cantilever length by just a factor of ten, it is not difficult to be in the opposite, SET back-action dominated regime. With, e.g.,  $V_g = 5$  V and  $Q_e = 10^4$ , we have  $Q_e/Q_i = 12$  and  $T_{\text{eff}} = T_i + 0.084 T_r \simeq T_i$  for  $T_r \ll 12 T_i$ .

## VII. CONCLUSIONS AND DISCUSSION

We have carried out a detailed analysis of the dynamics of a nano-mechanical resonator coupled to a SET. For the isolated SET-resonator system, the electrons tunnelling through the SET act like an effective thermal bath for the resonator. The variances of the stationary probability distribution for the resonator, and the dynamics associated

with its approach to the steady-state, allow us to assign an effective temperature and intrinsic damping constant due to the electrons, so long as the coupling between the resonator and the SET is small, i.e.,  $\kappa \ll 1$ .

The intrinsic damping constant controls the time taken for the isolated system to reach a steady-state. The effective temperature for the isolated SET-resonator system does not depend on the coupling between the resonator and the SET (for fixed values of  $\langle P \rangle_N$  and  $\langle P \rangle_{N+1}$ ), a fact which is somewhat surprising at first sight. However, although the average energy of the resonator in the steady-state is independent of the coupling,  $\kappa$ , the time taken for the energy stored in the resonator to reach this average, constant level is determined by the coupling. In the limit that the SET-resonator coupling goes to zero, the time taken to reach a steady-state will diverge and so the whole concept of a steady-state for the coupled system and hence an effective temperature breaks down. The effects of extrinsic damping can be understood as trying to take energy out of the resonator, through an additional pathway, on a time-scale set by the extrinsic damping rate. Hence, the effective temperature of the resonator will now depend on the relative magnitudes of the extrinsic and intrinsic damping constants.

We can also draw some conclusions from our results for the coupled dynamics which are more widely relevant to the study of nano-electromechanical systems. The idea that a mechanical resonator coupled to a mesoscopic conductor should have an intrinsic damping rate was demonstrated by Mozyrsky and Martin<sup>17</sup> and confirmed by Smirnov *et al.*<sup>22</sup> The results we obtain for a classical resonator demonstrate the generality of this result. Thus far, many studies of mesoscopic conductors coupled to nano-mechanical resonators<sup>8,10,38</sup> do not discuss the possibility of damping of the resonator arising from its interaction with the electrons. Indeed, in many nano-electromechanical systems it may be that there is a non-zero intrinsic damping rate which affects the character of the steady-state.

In this work, we have concentrated almost exclusively on how the properties of a nano-mechanical resonator are affected by coupling to a SET. Although we have calculated the effect of the coupling to the resonator on the average current through the SET, the spectrum of the current-noise has not yet been obtained, though work on this is in progress.<sup>39</sup> The current-noise spectrum will give important further information about the coupled dynamics of the system as it is very sensitive to correlations between the charge on the SET island and the position of the resonator.

While preparing this work we became aware of Ref. [40] which considers the quantum dynamics of the SET-resonator system, but in a different regime to that considered here.

### Acknowledgements

We would like to thank O. Buu, A. Korotkov, A. Martin, R. Onofrio, S. A. Ramakrishna, K. Schwab, and M. Wybourne for a number of very useful discussions. MPB and YZ were supported in part by an award from the Research Corporation, and by the National Security Agency (NSA) and Advanced Research and Development Activity (ARDA) under Army Research Office (ARO) Contract No. DAAG190110696.

## APPENDIX A: TOTAL ENERGY AND TUNNELLING RATES

The circuit diagram for a nano-mechanical resonator coupled capacitively to the island of a SET is shown schematically in Fig. 1, where a nano-mechanical resonator replaces the usual fixed voltage gate for the SET. In order to describe the dynamics of the coupled SET-resonator system, we require expressions for the total energy with  $N$  and  $N + 1$  electrons on the SET island as well as for the tunnelling rates through the two junctions.

### 1. Total energy

The total energy of the coupled SET-resonator system for a given number of charges on the island is most easily obtained by generalizing the usual expression for the energy of charges on an SET island with a fixed voltage gate,<sup>31</sup> given in Sec. II. Here we treat the resonator as a single-mode harmonic oscillator. The generalization to several modes is discussed in appendix C.

When the fixed gate is replaced by a harmonic oscillator, the gate capacitance, and hence the energy of the system, depends on the position of the oscillator. If the distance between the unperturbed oscillator and the SET island is  $d$  and the displacement,  $q$ , of the oscillator is always much less than this distance then the gate capacitance can be approximated by,

$$C_g(q) = C_g^0(1 - q/d) \quad (\text{A1})$$

where  $C_g^0$  is the capacitance of the un-displaced oscillator. Strictly-speaking we should write the approximation as  $C_g(q) = C_g^0 + q_0(dC_g/dq_0)_{q_0=0}$  where  $q_0$  is the normal mode displacement of the fundamental mode, but we will neglect this detail as it leads to an unimportant geometrical correction.

For nano-mechanical resonators, the values of  $C_g^0$  are typically much less than the SET junction capacitances  $C_j$ . Hence, we will neglect the position dependence of  $C_\Sigma$  and deal only with position dependence in the term  $-2NN_g$ . Thus, the charging energy of the SET island with  $N$  excess electrons can be written as,

$$E_{ch} = E_c \left( N^2 - 2NN_g^0 + 2NN_g^0 \frac{q}{d} \right), \quad (\text{A2})$$

where  $E_c = e^2/(2C_\Sigma)$  and  $N_g^0 = -C_g^0 V_g/e$  (for simplicity we will drop the superscripts from now on as  $N_g$  and  $C_g$  will always take this form in what follows).

The polarization charge induced by the gate can make the charging energies of states with  $N$  and  $N+1$  electrons on the SET island degenerate. For convenience, we define

$$\delta N = N_g - N - \frac{1}{2}. \quad (\text{A3})$$

Using this notation, we find

$$N^2 - 2NN_g = \delta N^2 + \frac{1}{4} + \delta N - N_g^2 \quad (\text{A4})$$

$$(N+1)^2 - 2(N+1)N_g = \delta N^2 + \frac{1}{4} - \delta N - N_g^2. \quad (\text{A5})$$

Thus, we can write the total energy of the coupled SET-resonator system with  $N$  and  $N+1$  excess electrons as,

$$H_N = E_c \delta N + 2E_c N_g \frac{q}{d} \left( N_g - \frac{1}{2} - \delta N \right) + \frac{p^2}{2m} + \frac{1}{2} m \omega_0^2 q^2 \quad (\text{A6})$$

$$H_{N+1} = -E_c \delta N + 2E_c N_g \frac{q}{d} \left( N_g + \frac{1}{2} - \delta N \right) + \frac{p^2}{2m} + \frac{1}{2} m \omega_0^2 q^2, \quad (\text{A7})$$

respectively, where we have dropped terms which are constant in both. Making the change of coordinates  $x = q + \Delta x$  to eliminate the linear term in  $H_N$ , we have

$$\frac{1}{2} m \omega_0^2 x^2 = \frac{1}{2} m \omega_0^2 q^2 + 2E_c N_g \frac{q}{d} \left( N_g - \delta N - \frac{1}{2} \right) + \frac{1}{2} m \omega_0^2 \Delta x^2, \quad (\text{A8})$$

where

$$\Delta x = \frac{2E_c N_g}{m \omega_0^2 d} \left( N_g - \delta N - \frac{1}{2} \right). \quad (\text{A9})$$

Expressing the total energies of the coupled system with  $N$  and  $N+1$  charges in terms of the new variable  $x$ , we obtain:

$$H_N = E_c \delta N + \frac{p^2}{2m} + \frac{1}{2} m \omega_0^2 x^2 \quad (\text{A10})$$

$$H_{N+1} = -E_c \delta N + \frac{p^2}{2m} + \frac{1}{2} m \omega_0^2 (x - x_0)^2 - \frac{1}{2} m \omega_0^2 x_0^2 - m \omega_0^2 x_0^2 (N_g - \delta N - 1/2), \quad (\text{A11})$$

where  $x_0 = -2E_c N_g/(m \omega_0^2 d)$  and we have again dropped constant terms.

## 2. Tunnelling rates

Within the orthodox model of single electron tunnelling, we can derive simple expressions for the tunnelling rates in either direction through the two SET junctions. Adopting the convention that electron tunnelling forwards corresponds to leftwards motion in Fig. 1, we can write down expressions for the four possible free energy differences:

$$\Delta E_L^+ = -\Delta E_L^- = H_{N+1} - H_N - \mu_L \quad (\text{A12})$$

$$\Delta E_R^+ = -\Delta E_R^- = H_N - H_{N+1} + \mu_R, \quad (\text{A13})$$

where  $\mu_{L(R)}$  is the chemical potential of the left(right)-hand lead. Using the expressions for  $H_N$  and  $H_{N+1}$  obtained above we find,

$$\Delta E_L^+ = -2E_c\delta N - m\omega_0^2 x_0 x - m\omega_0^2 x_0^2 (N_g - \delta N - 1/2) + \frac{eV_{ds}}{2} \quad (\text{A14})$$

$$\Delta E_R^+ = 2E_c\delta N + m\omega_0^2 x_0 x + m\omega_0^2 x_0^2 (N_g - \delta N - 1/2) + \frac{eV_{ds}}{2}, \quad (\text{A15})$$

where we have used the fact that  $-\mu_L = \mu_R = eV_{ds}/2$ .

## APPENDIX B: NUMERICAL INTEGRATION OF THE PROBABILITY DENSITY

In this appendix we outline the way in which the coupled master equations, (10) and (11), can be integrated numerically. The coupled equations of motion for the probability distributions contain terms describing the free evolution of the resonator, which are deterministic, and terms describing the tunnelling of electrons which are essentially stochastic. The free evolution of the resonator is known exactly and the problem of obtaining the dynamics of the overall distribution is simplified considerably by disentangling this part of the motion from the electron tunnelling by transforming to an interaction picture.

Formally, we can write the Liouville equation<sup>41</sup> for  $P_N(x, u; t)$ ,

$$i \frac{dP_N(x, u; t)}{dt} = L_N P_N(x, u; t), \quad (\text{B1})$$

where  $L_N$  is the Liouville operator and a very similar equation for  $P_{N+1}(x, u; t)$ . The dynamics of the resonator is simply that of a harmonic oscillator, albeit one whose equilibrium position shifts by  $x_0$  when an extra electron joins the island, together with a perturbation arising from tunnelling of electrons onto and off the island. Therefore, we can simplify the problem considerably by transforming into an interaction picture. We split the Liouville operator into two parts,

$$L_N = L_N^0 + \delta L, \quad (\text{B2})$$

where  $L_N^0 P_N(x, u; t) = i \{H_N, P_N(x, u; t)\}$  describes the free evolution of the oscillator with  $N$  charges on the island (for  $N+1$  charges, we define  $L_{N+1}^0 P_{N+1}(x, u; t) = i \{H_{N+1}, P_{N+1}(x, u; t)\}$  by analogy) and  $\delta L$  describes the electron tunnelling processes. Defining  $\tilde{P}_N(t) = e^{+iL_N^0 t} P_N(t)$ , and a similar relation for  $N+1$ , we have for the equations of motion in the interaction picture

$$\frac{d\tilde{P}_N(x, u; t)}{dt} = \frac{1}{Re^2} \{ \Theta[\Delta E_L^+(x')] \Delta E_L^+(x') + \Theta[\Delta E_R^-(x')] \Delta E_R^-(x') \} \quad (\text{B3})$$

$$\begin{aligned} & \times \tilde{P}_{N+1}(x + x_0(1 - \cos(\omega_0 t)), u + \omega_0 x_0 \sin(\omega_0 t); t) \\ & - \frac{1}{Re^2} \{ \Theta[\Delta E_R^+(x')] \Delta E_R^+(x') + \Theta[\Delta E_L^-(x')] \Delta E_L^-(x') \} \\ & \times \tilde{P}_N(x, u; t) \end{aligned} \quad (\text{B4})$$

$$\frac{d\tilde{P}_{N+1}(x, u; t)}{dt} = -\frac{1}{Re^2} \{ \Theta[\Delta E_R^+(x'')] \Delta E_R^+(x'') + \Theta[\Delta E_L^-(x'')] \Delta E_L^-(x'') \} \quad (\text{B5})$$

$$\begin{aligned} & \times \tilde{P}_{N+1}(x, u; t) \\ & + \frac{1}{Re^2} \{ \Theta[\Delta E_L^+(x'')] \Delta E_L^+(x'') + \Theta[\Delta E_R^-(x'')] \Delta E_R^-(x'') \} \\ & \times \tilde{P}_N(x - x_0(1 - \cos(\omega_0 t)), u - \omega_0 x_0 \sin(\omega_0 t); t) \end{aligned} \quad (\text{B6})$$

$$(\text{B7})$$

where

$$x' = \left[ x \cos(\omega_0 t) - \frac{u}{\omega_0} \sin(\omega_0 t) \right] \quad (\text{B8})$$

$$x'' = \left[ x_0 + (x - x_0) \cos(\omega_0 t) - \frac{u}{\omega_0} \sin(\omega_0 t) \right]. \quad (\text{B9})$$

Thus the transformation to the interaction picture eliminates the free-evolution of the oscillator and leaves us with a pair of simple rate equations which can be integrated numerically in a straightforward way.

Integrating these equations numerically on a finite grid and then performing the reverse transformation back from the interaction picture to obtain the full time dependence, we can calculate the probability distribution as a function of time. The accuracy of the calculation is set primarily by the size of the grid used, but convergence of the results can be confirmed by performing the calculation on grids with progressively smaller mesh sizes.

### APPENDIX C: HIGHER MODES OF THE RESONATOR

In the main body of this paper we treat the resonator as a single-mode harmonic oscillator and neglect the effect of all but the fundamental mode. In this appendix we show why such an approximate description works well.

In most studies of nano-electromechanical systems in which the mechanical component consists of a beam or cantilever, which has a spectrum of vibrational modes, all but the fundamental flexural mode is usually neglected. For systems where the coupling between modes is weak, this is a sensible approximation as it turns out that geometrical factors mean that the coupling between a normal mode of a beam or cantilever decreases rapidly with increasing frequency.<sup>15</sup>

In the system we consider here, the situation is a little different as the electrons passing through the SET act as a thermal bath and heat the resonator up to an effective temperature that is independent of the coupling. Therefore, in the absence of extrinsic damping each of the normal modes would have the same effective temperature. The overall variance in the position of the resonator would then be obtained by summing over the contribution from each of the normal modes. However, when we include the effect of external damping (discussed in Sec. IV,) it is found that the effective temperature for a single mode depends on the ratio of intrinsic to extrinsic damping rates:  $\gamma_i/\gamma_e$ . When the ratio  $\gamma_i/\gamma_e \ll 1$ , the extrinsic damping dominates and the SET has little effect on the mode. However, for  $\gamma_i/\gamma_e \leq 1$  the extrinsic damping does not fully counteract the thermal-like excitation of the mode due to the SET.

The intrinsic damping,  $\gamma_i$ , can be written in terms of the basic parameters of the system as

$$\gamma_i = \frac{Re^3}{md^2} \left( \frac{C_g V_g}{C_\Sigma V_{ds}} \right)^2. \quad (C1)$$

This formula follows from the approximation we made in appendix A where we neglected the distinction between the position of the center of mass of the resonator,  $q$ , and the normal-mode displacement of the fundamental mode. In fact, the linear correction to the gate capacitance should be written as  $(dC_g/dq_0)_{q_0=0} = -\chi C_g/d$ , where  $q_0$  is the fundamental mode position co-ordinate and  $\chi$  is a geometrical correction factor which we have neglected as it is of order unity for the fundamental mode.

In general, there will be an intrinsic damping constant for each normal mode of the resonator,  $n$ , of the form

$$\gamma_i^n = \frac{Re^3}{m} \left( \frac{V_g}{C_\Sigma V_{ds}} \right) \left( \frac{dC_g}{dq_n} \right)_{q_n=0}^2, \quad (C2)$$

where  $q_n$  is the displacement of the  $n$ -th normal mode.<sup>15,42</sup> However, the intrinsic damping constant for higher modes will always be *much less* than that of the fundamental mode because of their shorter wavelengths and the presence of nodes, which significantly reduce the value of the coupling, given by  $(dC_g/dq_n)_{q_n=0}$ .<sup>42</sup> Furthermore, there is reason to expect that the extrinsic damping,  $\gamma_e^n$ , will be greater for higher-frequency modes,<sup>43</sup> leading to a further reduction in the ratio  $\gamma_i^n/\gamma_e^n$ , and hence the effect of these modes on the overall motion of the resonator.

The current characteristics of the SET and the associated noise spectrum are also much more strongly affected by the fundamental mode of the resonator than by higher modes. This is again because of the weak-coupling between the resonator and the SET.

It should be noted that the treatment here could be extended to include the effect of higher modes of the resonator. The calculations presented in the main text consider a single mode, and the correct multi-mode results could easily be obtained by adding up the contributions of each of the modes, although the appropriate coupling constant,  $\kappa$  (which in general would depend on the frequency and geometry of the mode), would need to be used for each of the modes. The only assumption in our approach is that the normal modes of the resonator are effectively uncoupled from each other on all the time-scales of interest.

### APPENDIX D: PARAMETER VALUES

In this appendix we discuss the physical values of the various parameters in our model of the SET-resonator system which could be achieved using available technology. We concentrate on the parameter values which would be necessary

for the system to operate in the regime we have explored theoretically, where the SET is well-described by the orthodox model, and the drain-source voltage is large enough that the resonator behaves classically.

For the orthodox model to apply, the charging energy,  $E_c = e^2/(2C_\Sigma)$ , must dominate over the electron thermal energy scale,  $k_B T_e$ . The total capacitance of the SET,  $C_\Sigma$ , is dominated by the capacitance of the tunnel junctions,  $C_j$ , typically much larger than that of the mechanical gate,  $C_g$ . A typical choice of  $C_j = 0.25$  fF gives  $E_c/k_B \simeq 2$  K so that at electron temperatures of a few tens of mK, the charging energy clearly dominates. The junction resistances,  $R$ , of the SET must be set relatively high, e.g.,  $R = 100$  k $\Omega$ , in order to suppress higher-order electron tunnelling processes which cannot be described within the orthodox model. The drain-source voltage is typically chosen to be of order the charging energy  $eV_{ds} \sim e^2/(2C_\Sigma)$ , as it is in this regime that the SET conductance is most sensitive to changes in the gate capacitance. Thus for  $C_j = 0.25$  fF, we have, e.g.,  $V_{ds} = e/(2C_\Sigma) = 0.16$  mV and the electron tunnelling time,  $\tau_t$ , is consequently  $2RC_\Sigma = 10^{-10}$  s.

The properties of the nano-mechanical resonator used as a voltage-gate can be varied to quite a high degree. The frequency of a nano-mechanical resonator is determined by the material it is made from and its geometrical form. For a cantilever, a beam which is clamped at one end and free at the other, the fundamental flexural mode frequency is given by  $\omega_0 = 1.02(t/l^2)\sqrt{E/\rho}$ , where  $l$  is the length,  $t$  the thickness,  $E$  is Young's modulus, and  $\rho$  the mass density of the material from which the resonator is fabricated. Resonators fabricated from semiconductors typically have  $\sqrt{E/\rho}$  in the range<sup>45</sup>  $\sim 10^3$ – $10^4$  ms<sup>-1</sup>. For the example of a Si cantilever with  $E = 1.33 \times 10^{11}$  Nm<sup>-2</sup> and  $\rho = 2.33 \times 10^3$  kgm<sup>-3</sup>, the fundamental flexural mode frequency is  $f_0 = 1.2t/l^2$  GHz, with the dimensions expressed in micrometers. The gate capacitance of a nano-mechanical resonator is also determined by geometry. For a vacuum gap,  $C_g = \lambda\epsilon_0 lw/d$ , where  $w$  is the cantilever width,  $d$  the cantilever-SET island gap, and  $\lambda$  is a geometrical factor (which accounts, e.g., for the fact that the metal electrode may have smaller area than the cantilever surface  $lw$ ). Considering, e.g., a resonator with dimensions  $l = 1$   $\mu$ m,  $w = 0.25$   $\mu$ m,  $t = 0.2$   $\mu$ m,  $d = 0.1$   $\mu$ m, and  $\lambda = 1/3$ , we have  $C_g = 74$  aF and  $f_0 = 244$  MHz. This corresponds to  $\epsilon = 0.02$  for  $\tau_t = 10^{-10}$  s. The resonator would be well within the classical regime as the energy quanta for this frequency are  $\hbar\omega_0 = 0.15\mu$ eV, very much less than the energy associated with the above drain-source voltage.

The magnitude of the gate voltage,  $V_g$ , is limited by the need to avoid electrostatic breakdown in the dielectric between the SET and the resonator;<sup>14,19,44</sup> for vacuum the breakdown voltage is about  $10^8$  V/m,<sup>46</sup> translating into a maximum voltage of about 10 V for a resonator-SET island separation  $d = 0.1$   $\mu$ m.

- 
- <sup>1</sup> X.M.H. Huang, C.A. Zorman, M. Mehragany, and M.L. Roukes, *Nature (London)* **421**, 496 (2003).  
<sup>2</sup> M. Roukes, *Physics World* **14**, 25 (2001).  
<sup>3</sup> R.H. Blick, A. Erbe, L. Pescini, A. Kraus, D.V. Scheible, F.W. Beil, E. Hoehberger, A. Hoerner, J. Kirschbaum, H. Lorenz, and J.P. Kotthaus, *J. Phys. Cond. Matt.* **14**, R905 (2002).  
<sup>4</sup> A.N. Cleland and M.L. Roukes, *Nature (London)* **392**, 160 (1998).  
<sup>5</sup> J. Kirschbaum, E.M. Höhberger, R.H. Blick, W. Wegscheider, and M. Bichler, *Appl. Phys. Lett.* **81**, 280 (2002).  
<sup>6</sup> A.N. Cleland, J.S. Aldridge, D.C. Driscoll, and A.C. Gossard, *Appl. Phys. Lett.* **81**, 1699 (2002).  
<sup>7</sup> R.S. Knobel and A.N. Cleland, *Nature (London)* **424**, 291 (2003).  
<sup>8</sup> L.Y. Gorelik, A. Isacsson, M.V. Voinova, B. Kasemo, R.I. Shekhter, and M. Jonson, *Phys. Rev. Lett.* **80**, 4526. (1998); A. Isacsson, L.Y. Gorelik, M. V. Voinova, B. Kasemo, R.I. Shekhter, and M. Jonson, *Physica B* **255**, 150 (1998); T. Nord, L.Y. Gorelik, R.I. Shekhter, and M. Jonson, *Phys. Rev. B* **65**, 165312 (2002).  
<sup>9</sup> R.I. Shekhter, Yu. Galperin, L.Y. Gorelik, A. Isacsson, and M. Jonson, *J. Phys. Cond. Matt.* **15**, R441 (2003).  
<sup>10</sup> A.D. Armour and A. MacKinnon, *Phys. Rev. B* **66**, 035333 (2002).  
<sup>11</sup> N. Nishiguchi, *Phys. Rev. B* **65**, 035403 (2001).  
<sup>12</sup> A. Erbe, H. Krömmel, A. Kraus, R.H. Blick, G. Corso, and K. Richter, *App. Phys. Lett.* **77**, 3102 (2000).  
<sup>13</sup> R. Lifshitz and M.C. Cross, *Phys. Rev. B* **67**, 134302 (2003).  
<sup>14</sup> A.D. Armour, M.P. Blencowe, and K. C. Schwab, *Phys. Rev. Lett.* **88**, 148301 (2002).  
<sup>15</sup> A.D. Armour and M.P. Blencowe, *Phys. Rev. B* **64**, 035311 (2002).  
<sup>16</sup> M.P. Blencowe and M.N. Wybourne, *Physica B* **280**, 555 (2000).  
<sup>17</sup> D. Mozyrsky and I. Martin, *Phys. Rev. Lett.* **89**, 018301 (2002).  
<sup>18</sup> J.D. White, *Jap. J. Appl. Phys. Part 2* **32**, L1571-L1573 (1993).  
<sup>19</sup> M.P. Blencowe and M.N. Wybourne, *App. Phys. Lett.* **77**, 3845 (2000).  
<sup>20</sup> Y. Zhang and M.P. Blencowe, *J. Appl. Phys.* **91**, 4249 (2002).  
<sup>21</sup> V. B. Braginsky and F. Ya. Khalili, *Quantum Measurement*, (Cambridge University Press, Cambridge, UK, 1992).  
<sup>22</sup> A.Yu. Smirnov, L.G. Mourokh, and N.J.M. Horing, *Phys. Rev. B* **67**, 115312 (2003).  
<sup>23</sup> A.O. Caldeira and A.J. Leggett, *Ann. Phys. (NY)* **149**, 374 (1983).  
<sup>24</sup> Note, however, within the framework of our classical description of the SET, the electron temperature cannot be arbitrarily small as discussed by H. Schoeller and G. Schön, *Phys. Rev. B* **50**, 18436 (1994).  
<sup>25</sup> R.L. Kautz, G. Zimmerli, and J.M. Martinis, *J. Appl. Phys.* **73**, 2386 (1993).

- <sup>26</sup> A.N. Korotkov, M.R. Samuelsen, and S.A. Vasenko, J. Appl. Phys. **76**, 3623 (1994).
- <sup>27</sup> M.H. Devoret and R.J. Schoelkopf, Nature (London) **406**, 1039 (2000).
- <sup>28</sup> R.J. Schoelkopf, P. Wahlgren, A.A. Delsing, and D. Prober, Science **280**, 1238 (1998).
- <sup>29</sup> K.W. Lehnert, K. Bladh, L.F. Spietz, D. Gunnarsson, D.I. Schuster, P. Delsing, and R.J. Schoelkopf, Phys. Rev. Lett. **90**, 027002 (2003).
- <sup>30</sup> D.K. Ferry and S.M. Goodnick, *Transport in Nanostructures*, (Cambridge University Press, Cambridge, UK, 1997).
- <sup>31</sup> A. Shnirman and G. Schön, Phys. Rev. B **57**, 15400 (1998); Y. Makhlin, G. Schön and A. Shnirman, Rev. Mod. Phys. **73**, 357 (2001).
- <sup>32</sup> M. Amman, R. Wilkins, E. Ben-Jacob, P.D. Maker, and R.C. Jaklevic, Phys. Rev. B **43**, 1146 (1991).
- <sup>33</sup> D.S. Lemons, *An Introduction to Stochastic Processes*, (John Hopkins University Press, Baltimore, MD, 2002).
- <sup>34</sup> A.N. Cleland *Fundamentals of Nanomechanics*, (Springer-Verlag, Heidelberg, Germany, 2002).
- <sup>35</sup> H. Hirakawa, S. Hiramatsu, and Y. Ogawa, Phys. Lett. A **63** 199 (1977).
- <sup>36</sup> Y. Zhang *et al.*, (in preparation).
- <sup>37</sup> M.L. Roukes, Tech. Digest 2000 Solid-State Sensor and Actuator Workshop, Transducer Research Foundation, Cleveland, 2000; cond-mat/0008187.
- <sup>38</sup> T. Brandes and N. Lambert, Phys. Rev. B **67**, 125323 (2003).
- <sup>39</sup> A.D. Armour and M.P. Blencowe, (in preparation)
- <sup>40</sup> D. Mozyrsky, I. Martin, and M.B. Hastings, cond-mat/0306480.
- <sup>41</sup> I. Prigogine, *Non-Equilibrium Statistical Mechanics*, (Interscience, John Wiley, NY, 1962).
- <sup>42</sup> H.-J. Butt and M. Jaschke, Nanotechnology **6**, 1 (1995).
- <sup>43</sup> S. Rast, C. Wattinger, U. Gysin, and E. Meyer, Nanotechnology **11**, 169 (2000).
- <sup>44</sup> K.C. Schwab, Appl. Phys. Lett. **80**, 1276 (2002).
- <sup>45</sup> Y.T. Yang, K.L. Ekinci, X.M.H. Huang, L.M. Schiavone, M.L. Roukes, C.A. Zorman, and M. Mehragany, Appl. Phys. Lett. **78**, 162 (2001).
- <sup>46</sup> X. Ma and T.S. Sudarshan, J. Vac. Sci. Technol. B **16**, 1174 (1998).